

# The origin of the mass discrepancy–acceleration relation in $\Lambda$ CDM

Julio F. Navarro<sup>1\*</sup>, Alejandro Benítez-Llambay<sup>2</sup>, Azadeh Fattahi<sup>1</sup>,  
 Carlos S. Frenk<sup>2</sup>, Aaron D. Ludlow<sup>2</sup>, Kyle A. Oman<sup>1</sup>, Matthieu Schaller<sup>2</sup>,  
 Tom Theuns<sup>2</sup>.

<sup>1</sup>*Department of Physics and Astronomy, University of Victoria, Victoria, BC, Canada V8P 5C2*

<sup>2</sup>*Institute for Computational Cosmology, Department of Physics, Durham University, South Road, Durham, DH1 3LE, UK*

<sup>3</sup>*Leiden Observatory, Leiden University, PO Box 9513, 2300 RA Leiden, The Netherlands*

Accepted XXX. Received YYY; in original form ZZZ

## ABSTRACT

We examine the origin of the mass discrepancy–radial acceleration relation (MDAR) of disk galaxies. This is a tight empirical correlation between the disk centripetal acceleration and that expected from the baryonic component. The MDAR holds for most radii probed by disk kinematic tracers, regardless of galaxy mass or surface brightness. The relation has two characteristic accelerations;  $a_0$ , above which all galaxies are baryon-dominated; and  $a_{\min}$ , an effective minimum acceleration probed by kinematic tracers in isolated galaxies. We use a simple model to show that these trends arise naturally in  $\Lambda$ CDM. This is because: (i) disk galaxies in  $\Lambda$ CDM form at the centre of dark matter haloes spanning a relatively narrow range of virial mass; (ii) cold dark matter halo acceleration profiles are self-similar and have a broad maximum at the centre, reaching values bracketed precisely by  $a_{\min}$  and  $a_0$  in that mass range; and (iii) halo mass and galaxy size scale relatively tightly with the baryonic mass of a galaxy in any successful  $\Lambda$ CDM galaxy formation model. Explaining the MDAR in  $\Lambda$ CDM does not require modifications to the cuspy inner mass profiles of dark halos, although these may help to understand the detailed rotation curves of some dwarf galaxies and the origin of extreme outliers from the main relation. The MDAR is just a reflection of the self-similar nature of cold dark matter haloes and of the physical scales introduced by the galaxy formation process.

**Key words:** dark matter – galaxies: kinematics and dynamics – galaxies: structure

## 1 INTRODUCTION

The outer rotation curves of disk galaxies clearly deviate from Newtonian predictions based on the gravitational attraction of their gaseous and stellar components (Rubin et al. 1978; Bosma 1978). These deviations are usually ascribed to massive, spatially extended dark matter haloes, a conclusion strongly supported by independent lines of evidence, such as gravitational lensing of background objects by galaxies and clusters, as well as by the structure of the Doppler peaks in the cosmic microwave background, which suggests that most matter in the Universe is in some non-baryonic form that interacts little with radiation. A review of the topic may be found in Bertone et al. (2005) and a summary of the latest parameters inferred from cosmolog-

ical surveys may be found in Planck Collaboration et al. (2016).

Although the evidence for dark matter seems on balance overwhelming, a number of curious features in the kinematic evidence for dark matter in disk galaxies have attracted attention over the years. These have been argued to challenge the dark matter interpretation of the data, and have motivated work on alternative theories of gravity. Popular amongst them is the idea that Newtonian gravity breaks down in the regime of ‘low acceleration’ ( $a < a_0 \sim 10^{-10} \text{ m s}^{-2}$ ) reached in the outskirts of galaxy disks, as in the MOND scenario proposed by Milgrom (1983).

A chief attraction of this idea is that disk rotation curves show *obvious* deviations from Newtonian predictions only in that regime, regardless of other properties of the galaxy, such as mass, surface brightness, or gas content (Sanders 1990).

\* E-mail: jfn@uvic.ca

Furthermore, the amount of dark matter needed to explain, at a given radius, the observed rotation velocity seems to correlate strongly with the enclosed baryonic mass, to the extent that the full rotation curve of most disks may often be predicted solely from the spatial distribution of baryons (see, e.g., Scarpa 2006; Wu & Kroupa 2015, and references therein). This is an intriguing result, which has at times been ascribed to a ‘conspiracy’ between the disk and the halo, but which has also strengthened alternative theories such as MOND, where such correlations are thought to arise more naturally.

These issues have been revisited recently by McGaugh et al. (2016) and Lelli et al. (2016b) using a compilation of late-type galaxy rotation curves and  $3.6\ \mu\text{m}$  Spitzer photometry, the band where uncertainties in the stellar mass-to-light ratio are minimized (Bell & de Jong 2001). These authors show that, for galaxies in their sample, the disk centripetal acceleration,  $g_{\text{tot}}(r) = V_{\text{circ}}^2(r)/r$ , correlates strongly with that inferred from the spatial distribution of the baryonic component,  $g_{\text{bar}}(r)$ , a relation termed ‘the mass discrepancy–radial acceleration relation’, or MDAR for short.

The MDAR indicates that baryons dominate in regions of high acceleration; i.e.,  $g_{\text{tot}} \approx g_{\text{bar}}$  when  $g_{\text{tot}} > a_0$ . In addition, few galaxies probe accelerations below a well defined minimum value of  $a_{\text{min}} \sim 10^{-11}\ \text{m s}^{-2}$ . The latter point is further strengthened when adding to the sample the ultra-faint satellites of the Milky Way, which include some of the most dark matter-dominated and lowest-acceleration galaxies known (Lelli et al. 2016a).

These results have renewed interest in the origin of the MDAR, and in its theoretical interpretation. Although some have argued that the MDAR is tantamount to a natural law that requires ‘new physics’ (e.g., Famaey & McGaugh 2012; Kroupa 2012; McGaugh 2015), others have claimed that the MDAR arises as a consequence of the scaling relations between the size and mass of galaxies and dark haloes in the current paradigm of structure formation,  $\Lambda\text{CDM}$  (Di Cintio & Lelli 2016; Keller & Wadsley 2016; Ludlow et al. 2016a; Desmond 2016).

It is clear from the current debate, however, that for the latter interpretation to gain wide acceptance the reason for the existence of characteristic accelerations such as  $a_0$  and  $a_{\text{min}}$  in disk kinematic data must be clearly identified. Our aim is therefore to outline a simple argument for the origin of the MDAR within the  $\Lambda\text{CDM}$  framework, including a compelling motivation for its asymptotic behavior and for the characteristic accelerations imprinted in it.

Our contribution extends earlier work, such as that of van den Bosch & Dalcanton (2000), who used a semi-analytic model to show that the MDAR may be reproduced in  $\Lambda\text{CDM}$  when galaxies are constrained to match the Tully-Fisher relation, or that of Kaplinghat & Turner (2002), who used cosmological arguments to motivate the origin of  $a_0$ . These arguments point to a well-defined link between the ‘allowed’ combinations of size, stellar and total mass of galaxies and the narrow scatter of the MDAR, which we develop further below.

## 2 THE MODEL

In  $\Lambda\text{CDM}$ , galaxies form at the centre of dark matter haloes whose structural parameters and mass profiles are well understood (Navarro et al. 1996, 1997, hereafter, NFW). A large body of numerical work has shown that cold dark matter haloes are well approximated by NFW profiles, and may be characterized by two parameters, usually expressed as a virial<sup>1</sup> mass and a ‘concentration’ parameter relating the characteristic radius of a halo,  $r_s$ , to its virial radius,  $c = r_{200}/r_s$ . These two parameters are not independent. The  $M_{200}(c)$  relation and its dependence on cosmological parameters is now well understood (see Ludlow et al. 2014, 2016b, and references therein), and therefore the full mass profile of a  $\Lambda\text{CDM}$  halo is known once its virial mass is specified.

In this context, the simplest galaxy formation model that may be used to examine the MDAR requires the choice of a baryonic (stellar) mass ( $M_{\text{str}}$ ), a size and radial profile, as well as a way to relate stellar mass to halo mass. The latter is probably the best understood of those ingredients, given the strong constraint placed by the galaxy stellar mass function on the halo mass–stellar mass relation in  $\Lambda\text{CDM}$ . (We use ‘stellar’ or ‘baryonic’ indistinctly to refer to the mass of the luminous component in this simple model.)

A simple, but reasonably accurate, parametrization of that relation is provided by ‘abundance-matching’ models, where galaxies are assigned to dark matter haloes respecting their relative rankings by mass (Frenk et al. 1988; Vale & Ostriker 2004; Guo et al. 2010; Behroozi et al. 2013; Moster et al. 2013). The solid line in the left panel of Fig. 1 indicates the relation derived by Behroozi et al. (2013) and compares it with the results of the EAGLE and APOSTLE cosmological hydrodynamical simulations<sup>2</sup> (Schaye et al. 2015; Crain et al. 2015; Sawala et al. 2016; Fattahi et al. 2016). These simulations have been shown to match reasonably well the galaxy stellar mass function over more than 4 decades in stellar mass; the shape of disk galaxy rotation curves (Schaller et al. 2015); and the zero-point, slope, and scatter of the Tully-Fisher relation (Ferrero et al. 2016). Note that the stellar mass–halo mass relation is rather steep at the faint end, implying that there is, broadly speaking, an effective ‘minimum’ halo mass required for a luminous galaxy to form (see, e.g., Sawala et al. 2016; Benítez-Llambay et al. 2016, for further discussion).

Galaxy sizes are known empirically to scale with stellar mass, as shown, for example, by the SPARC sample of Lelli et al. (2016b, filled squares in the right-hand panel of Fig. 1). EAGLE and APOSTLE galaxies match the stellar half-mass radius ( $r_h$ ) of SPARC galaxies fairly well, especially for galaxies more massive than a few times  $10^7 M_\odot$ . To first order,  $r_h$  is well approximated by the relation  $r_h = 0.2 r_s$ , as illustrated by the solid line in the right-hand panel of Fig 1.

<sup>1</sup> Virial quantities correspond to those of the sphere where the enclosed mean density is 200 times the critical density for closure,  $\rho_{\text{crit}} = 3H_0^2/8\pi G$ , and are identified with a 200 subscript.

<sup>2</sup> We show the results of the Ref-L025N0752 run of the EAGLE project, and L1 and L2 runs of APOSTLE. The EAGLE and APOSTLE-L2 runs have similar resolution, with gas particle mass of  $\sim 10^5 M_\odot$ , while the APOSTLE-L1 runs have  $10\times$  better mass resolution, i.e.  $\sim 10^4 M_\odot$  per gas particle. All runs use the same subgrid physical model.

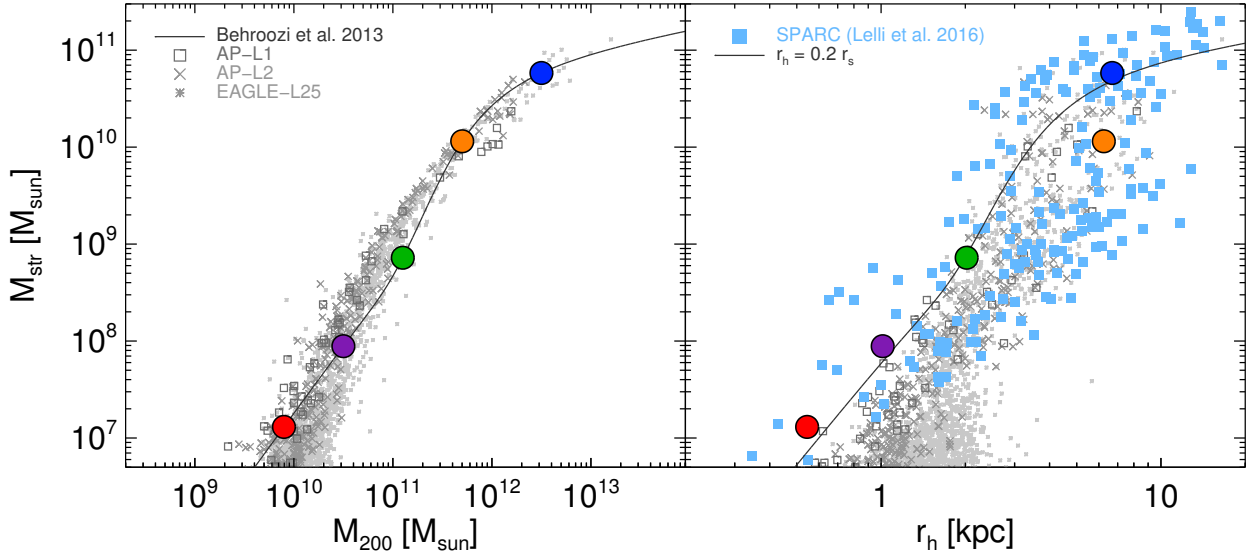


**Figure 1.** *Left:* Stellar mass vs. halo mass of five galaxies (solid circles), chosen to follow the abundance-matching relation of Behroozi et al. (2013). Simulated galaxies from the EAGLE (Ref-L025N0752), APOSTLE-L1, and APOSTLE-L2 simulations are shown with asterisks, crosses, and open squares, respectively. The total stellar mass of the simulated galaxies ( $M_{\text{str}}$ ) corresponds to all bound star particles within a radius  $r_{\text{gal}} = 0.15 r_{200}$ . *Right:* Stellar mass vs. 3D stellar half-mass radii ( $r_h$ ). For the galaxy models we choose radii so that their characteristic accelerations follow the observed MDAR (see top-left panel of Fig. 2). The solid line indicates  $r_h = 0.2 r_s$ , for reference. The stellar mass vs.  $r_h$  relation of model galaxies that match the MDAR is broadly consistent with the SPARC sample of galaxies. We assume  $r_h = (4/3)R_{\text{eff}}$  for the SPARC sample to account for projection effects.

These two relations show that in  $\Lambda$ CDM stellar masses and sizes are inextricably linked to the masses and sizes of their surrounding haloes.

The final choice of our model is a radial mass profile for the stellar (baryonic) component of a galaxy, for which we adopt an exponential surface density profile,

$$\Sigma_{\text{bar}}(r) = \Sigma_0 e^{-r/r_d}, \quad (1)$$

where  $r_d = r_h/1.678$  is the exponential scale radius and the total disk mass is  $M_{\text{str}} = 2\pi\Sigma_0 r_d^2$ . This is a good approximation to the spatial distribution of stars in a typical galaxy disk.

The total acceleration profile of the galaxy,  $g_{\text{tot}}(r)$ , may then be calculated from the contributions of dark matter and stars,

$$g_{\text{tot}}(r) = g_{\text{dm}}(r) + g_{\text{bar}}(r) = GM_{\text{dm}}(< r)/r^2 + V_{\text{bar}}(r)^2/r, \quad (2)$$

where  $G$  is the gravitational constant;  $M_{\text{dm}}(< r)$  is the enclosed mass of an NFW halo, corrected by a factor<sup>3</sup>  $(1 - \Omega_{\text{bar}}/\Omega_{\text{m}}) = 0.84$  to account for the universal baryon fraction, and  $g_{\text{bar}}(r) = V_{\text{bar}}(r)^2/r$  is the contribution of the baryons to the centripetal acceleration.

Note that the dark matter contribution has a characteristic acceleration, given by the central (maximum) value of an NFW profile:  $g_{\text{dm}}^{\text{max}} = [c^2/(\ln(1+c) - c/(1+c))] (V_{200}^2/2r_{200})$ . The baryons

also have a well defined maximum acceleration,  $g_{\text{bar}}^{\text{max}} = 0.286 GM_{\text{str}}/r_d^2$ , which occurs at  $r_{\text{bar}}^{\text{max}} = 0.747 r_d$ .

Each galaxy in our model therefore has a characteristic acceleration,  $g_{\text{tot}}^{\text{max}}$ , given by the sum of these two values. Note that  $g_{\text{dm}}$  and  $g_{\text{bar}}$  might peak at different radii so, for simplicity, we shall adopt the total and baryonic accelerations at  $r_{\text{bar}}^{\text{max}}$  as the characteristic values for a model galaxy. In practice,  $g_{\text{tot}}^{\text{max}} \approx g_{\text{tot}}(r_{\text{bar}}^{\text{max}})$  so this choice makes no difference to any of our results.

Finally, we have chosen to neglect here the response of the halo to the assembly of the galaxy, mainly for simplicity but also because there is still no overall consensus on the magnitude or even sign (i.e., contraction or expansion) of the effect.

### 3 RESULTS

#### 3.1 MDAR and scaling relations

Disk rotation curves are best constrained around the baryonic half-mass radius, where kinematic tracers are most abundant. For our model to be successful galaxies must therefore have characteristic accelerations ( $g_{\text{tot}}^{\text{max}}$  and  $g_{\text{bar}}^{\text{max}}$ ) that follow the MDAR. This condition places strong constraints on the relation between galaxy stellar mass, size, and the mass of its surrounding halo. We illustrate this in the top-left panel of Fig. 2, where the filled circles correspond to five example galaxies selected to follow the abundance matching relation and to have radii so that their characteristic accelerations lie on the MDAR. These examples span a range of nearly four decades in stellar mass and more than one decade in radius. Their halo masses are taken from the

<sup>3</sup> Cosmological parameters adopted throughout the paper are according to the Planck results  $\Omega_{\text{m}} = 0.307$ ,  $\Omega_{\Lambda} = 0.693$ ,  $\Omega_{\text{bar}} = 0.04825$ , and  $H_0 = 67.77 \text{ km s}^{-1} \text{ Mpc}^{-1}$  (Planck Collaboration et al. 2014).

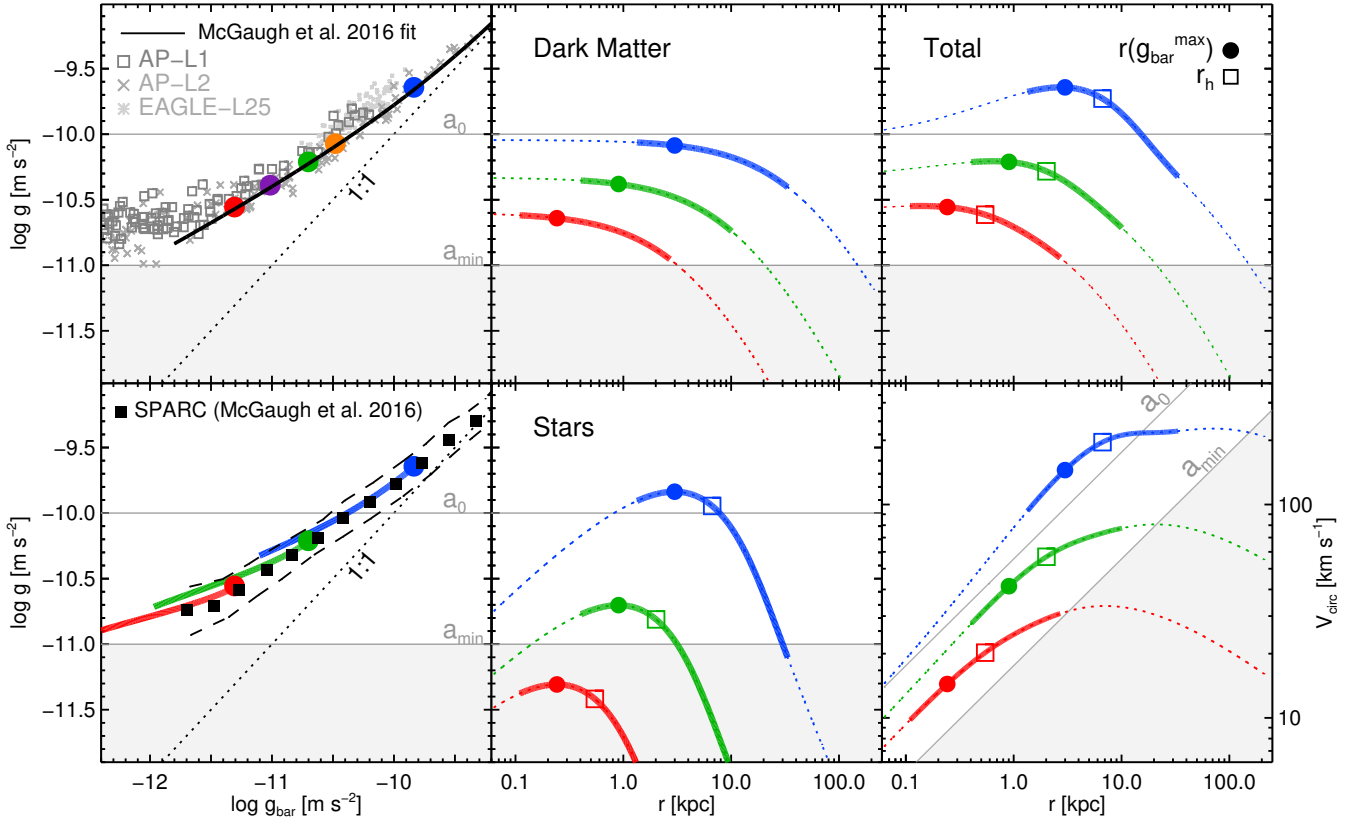


**Figure 2.** *Top-left:* Characteristic accelerations of the five model galaxies shown in Fig. 1 (i.e.,  $g_{\text{bar}}^{\text{max}}$  and  $g_{\text{tot}}^{\text{max}}$ ; filled circles) whose parameters have been chosen to match the MDAR of McGaugh et al. (2016) (solid black line). Each simulated APOSTLE/EAGLE galaxy is shown once, evaluated at the stellar half-mass radius. *Bottom-left:* Same as top-left, but showing the radial acceleration profiles of three of the five model galaxies (for clarity). The radial range shown extends from  $0.2 r_h$  to  $5 r_h$  (thick lines). Filled circles are as in the top-left in all panels. The filled squares and dashed lines indicate the same MDAR (and its scatter) of McGaugh et al. (2016). *Top-middle:* Acceleration profiles,  $g_{\text{dm}}$ , of the dark haloes of three of the models shown in the top-left panel. Dark matter haloes are assumed to follow NFW profiles, which have a broad maximum at the centre. *Bottom-middle:* Contribution of the baryons,  $g_{\text{bar}}$ , to the acceleration profile in our galaxy models. For exponential disk stellar mass distributions, the acceleration reaches a characteristic maximum value of  $g_{\text{bar}}^{\text{max}}$  at  $0.45 r_h$  (filled circles). Open squares indicate the stellar half-mass radius. *Top-right:* Same as middle panels, but for dark matter + baryonic components. *Bottom-right:* Total circular velocity profiles of our models. See right-hand axis for units. In all panels the thick solid lines represent the radial range from  $0.2 r_h$  to  $5 r_h$ , and the open squares mark  $r_h$ . The shaded grey regions correspond to total acceleration below  $a_{\text{min}} = 10^{-11} \text{ m s}^{-2}$ . These regions are excluded for isolated galaxies, according to our simple model of galaxy formation in  $\Lambda\text{CDM}$ . See text for a full discussion.

Behroozi et al. (2013) model, and their NFW concentrations from the recent work of Ludlow et al. (2016b).

The example galaxies have radii quite consistent with the SPARC mass-size relation, as may be seen in the right-hand panel of Fig. 1. This shows that  $\Lambda\text{CDM}$  galaxies that follow *simultaneously* the abundance-matching prescription (needed to match the galaxy stellar mass function) and the empirical mass-size relation can reproduce the observed MDAR without further adjustment.

The MDAR thus results largely from the scaling relations linking the size and mass of disk galaxies with the mass of their surrounding halos. Indeed, the slight offset between the observed MDAR and that of APOSTLE and EAGLE (top-left panel of Fig. 2) may be traced to the slight and systematic deviations of simulated galaxies from both the abundance-matching and the empirical mass-size relations (see Fig. 1 and the discussion in Ludlow et al. 2016a).

### 3.2 The origin of $a_0$ and $a_{\text{min}}$

The middle panels of Fig. 2 explain the origin of the two MDAR characteristic parameters;  $a_0$  and  $a_{\text{min}}$ , which, in  $\Lambda\text{CDM}$ , result from the following considerations: (i) the NFW acceleration profile has a well-defined maximum central value, and declines very gradually with radius near the centre; (ii) the peak acceleration varies by *only* a factor of  $\sim 4$  for galaxies that differ by a factor of  $\sim 10^4$  in stellar mass; (iii) the peak acceleration of the halo that hosts the most massive galaxy is very nearly  $a_0 \approx 10^{-10} \text{ m s}^{-2}$ ; and (iv) the minimum acceleration  $a_{\text{min}}$  coincides with the NFW acceleration at the outer edge (i.e.,  $r \sim 5 r_h$ ) of the faintest galaxy in the examples.

Note that these results do not require any parameter tuning or complicated galaxy formation model. They just rely on: (a) the NFW mass profile shape, which has a well-defined, broad acceleration maximum at the centre; (b) a

reasonably tight correlation between stellar mass and halo mass that satisfies the galaxy stellar mass function; and (c) the limited radial range probed by luminous kinematic tracers in galaxies.

Requisite (a) is a defining characteristic of  $\Lambda$ CDM haloes, and one that does not necessarily hold for alternative dark matter models. The peak accelerations in  $\Lambda$ CDM haloes are determined by the cosmological parameters, which, unlike more ad-hoc proposals like MOND, have *not* been tuned to fit rotation curve data.

Condition (b) is a crucial outcome of any successful  $\Lambda$ CDM galaxy formation model, and it is a result of the baryon-driven energetic processes that regulate galaxy formation. These processes select a characteristic halo mass range outside of which galaxy formation becomes extremely inefficient: at the centre of massive cluster-sized halos, for example, where AGN feedback and long cooling times limit galaxy growth, and in low-mass haloes, where the heating from cosmic reionization and supernova feedback impose an effective minimum mass for halos that host luminous galaxies. Galaxies in  $\Lambda$ CDM (and especially disks) thus form in a narrow range of halo virial velocity and an even narrower range of central accelerations.

Finally, condition (c) is also important, since it predicts that extending observations to radii well beyond the inner halo regions should lead to systematic deviations from the MDAR.

The asymptotic behaviour of the  $g_{\text{tot}}-g_{\text{bar}}$  relation can be simply understood from the above discussion. Firstly, accelerations larger than  $a_0$  can *only* be reached in regions where baryons (which may contract dissipatively and reach high densities/accelerations) dominate. At accelerations greater than  $a_0$ , then, one expects  $g_{\text{tot}} \approx g_{\text{bar}}$ , regardless of any other galaxy property.

In regions where dark matter dominates, disk accelerations cannot drop below  $a_{\text{min}}$ , since that is roughly the minimum acceleration traced in the observationally accessible range of the lowest mass haloes that are effectively able to host a luminous isolated galaxy. The model also predicts that dark matter-dominated dwarfs should have acceleration profiles that vary weakly with radius, approaching a constant  $g_{\text{tot}} \sim a_{\text{min}}$  at very low values of  $g_{\text{bar}}$ .

We emphasize that the latter conclusion applies only to isolated ‘field’ dwarfs, and *not* to satellite galaxies, which may see their mass reduced by tidal stripping. Indeed, tidally stripped satellites are expected to probe total acceleration values significantly below  $a_{\text{min}}$ , as in the case of the recently discovered Milky Way satellite Crater II (Caldwell et al. 2017). The relatively large size of this satellite and its extremely low velocity dispersion are indicative of extremely low accelerations;  $g_{\text{tot}} \sim 6 \times 10^{-13} \text{ m s}^{-2}$ . Such extreme departure from the minimum expected for field dwarfs in  $\Lambda$ CDM suggests that Crater II must have been undergone large amounts of tidal stripping, probably affecting both its dark matter and stellar components. We plan to examine the consistency of this hypothesis with observations of the Local Group satellite population in a separate contribution.

### 3.3 MDAR and radial profiles

According to McGaugh et al. (2016) and Lelli et al. (2016b), the MDAR also appears to hold at various radii of individ-

ual galaxies, an issue we address in the remaining panels of Fig. 2. The top right panel shows the centripetal acceleration profile,  $g_{\text{tot}}(r)$ , of our example galaxies (only three out of five are shown for clarity). The profiles are shown in thick solid line type over the radial range typically covered by kinematic tracers; from 20 per cent of  $r_{\text{h}}$  to  $5 \times r_{\text{h}}$ . (For reference, this corresponds to  $\sim 0.7\text{--}18$  kpc for a galaxy like the Milky Way; see, e.g., Bovy & Rix 2013). The filled circle indicates the characteristic acceleration of the galaxy; i.e., the acceleration at the radius where  $g_{\text{bar}}(r)$  peaks (see bottom middle panel of Fig. 2).

Because the halo acceleration has a central maximum, and because the peak baryonic acceleration occurs inside  $r_{\text{h}}$ , neither the dark matter nor the disk acceleration vary substantially over a wide radial range, especially near the centre. This implies that the rotation curve of an individual galaxy contributes many points to the MDAR just around the characteristic value indicated by the solid circle in the left panels of Fig. 2. This is in part responsible for the small scatter reported for the MDAR, to an extent that depends on exactly how the radial profile of individual galaxies is sampled, an issue to which we shall return below.

Outside  $r_{\text{h}}$ , the baryonic acceleration profile declines rapidly with radius, extending the imprint of individual galaxies on the MDAR to the left of each solid circle and following approximately the average MDAR, as shown in the bottom-left panel of Fig. 2.

In systems where dark matter dominates (i.e., faint, low surface brightness galaxies like the one identified in red) the total acceleration changes little over the radial range where kinematic tracers are present, explaining why the relation becomes nearly horizontal at very small values of  $g_{\text{bar}}$ .

On the other hand, in more massive, higher surface brightness systems that are less baryon dominated (like the one identified in blue in Fig. 2) the outer decline of the baryonic acceleration profile is more pronounced, and leads to a steeper dependence of  $g_{\text{tot}}$  with  $g_{\text{bar}}$  in the outer<sup>4</sup> regions. The combination of these effects explains quite well the observed MDAR, as shown in the bottom-left panel of Fig. 2.

### 3.4 MDAR and dark matter ‘cores’

The previous discussion demonstrates that there is no need to appeal to constant density ‘cores’ in the inner dark matter profile to explain the MDAR in  $\Lambda$ CDM, in agreement with the conclusions of earlier work (see, e.g., Di Cintio & Lelli 2016; Keller & Wadsley 2016; Ludlow et al. 2016a; Desmond 2016). Baryon-induced cores may be useful, however, to explain some outlier points in the relation, such as those contributed by the inner regions of galaxies whose rotation curves suggest the presence of a core in the dark matter density profile—such cores are not included in our simple model. Baryon-induced cores have also been argued to improve agreement with the observed MDAR in the low-mass galaxy regime, but the improvements refer to a small

<sup>4</sup> Note that  $g_{\text{tot}}$  also declines towards the centre in systems where the disk dominates. This just reflects the importance of the disk in the overall potential and should not be confused with the presence of a constant density ‘core’ in the dark matter, which may result in a similar trend in dark-matter dominated systems.

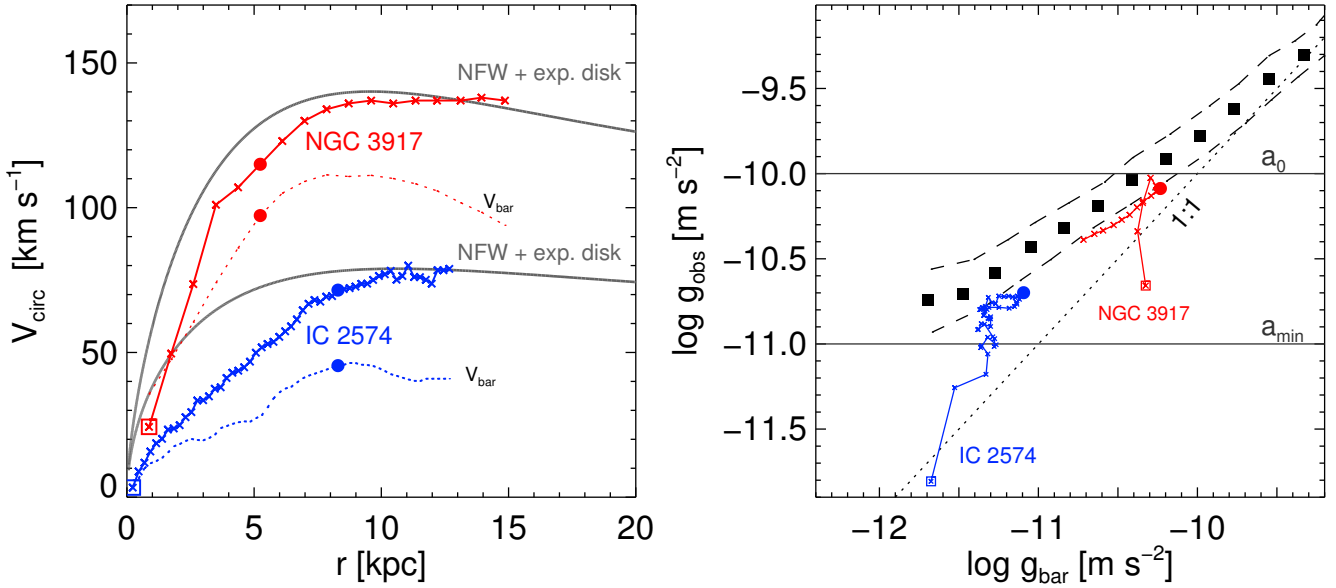


**Figure 3.** Illustration of the effect on the MDAR of alleged ‘cores’ in the inner dark matter density profiles. *Left:* Rotation curves of two galaxies with large inner mass deficits. Lines connecting symbols are the inferred rotation curves; dotted lines are the contribution of the baryonic components. Filled circles indicate the location of the peak in the baryonic acceleration profile,  $g_{\text{bar}}(r)$ . Thin grey lines are the result of our model, chosen to match the peak in the baryonic circular velocity profile, and the maximum rotation velocity of each galaxy. *Right:* The same two galaxies in the MDAR. Note that the inner regions, where the cores prevail, deviate systematically from the average MDAR. See text for further discussion.

fraction of outlier points and do not alter the main relation, at least for a core-formation model like that of Di Cintio & Lelli (2016, see their fig. 4).

We illustrate the effect of cores in the MDAR by using data for two galaxies whose rotation curves show an inner deficit of mass compared with the predictions of  $\Lambda\text{CDM}$  models. As discussed by Oman et al. (2015), this deficit is a robust characterization of the ‘core vs cusp’ controversy, as shown in Fig. 3 for NGC 3917 (Lelli et al. 2016b) and IC 2574 (Walter et al. 2008; Oh et al. 2011). The rotation curve data are compared with the predictions of our simple model (grey lines), after choosing disk and halo parameters to match the peak in the baryonic circular velocity profile and the maximum observed rotation velocity of each galaxy. Assuming that the rotation curves faithfully trace the circular velocity profiles, the alleged ‘cores’ show up as a mismatch in the inner velocity profiles of model and observation. These galaxies are two fairly extreme examples of alleged cores, but are useful to illustrate the point.

As shown in the right-hand panel of Fig. 3, although the characteristic accelerations of these two galaxies are not far from the mean MDAR (filled circles), their inner regions show large systematic deviations, even contributing a few points to the MDAR that dip below the minimum acceleration  $a_{\text{min}}$  discussed in Sec. 3.2. Baryon-induced cores may help to explain these outliers, but are not critical to the origin of the main MDAR trend in  $\Lambda\text{CDM}$ , which is delineated by the relation between the characteristic accelerations  $g_{\text{tot}}^{\text{max}}$  and  $g_{\text{bar}}^{\text{max}}$  discussed in Sec. 3.1.

We also note that the MDAR outliers arise from acceleration estimates very near the galaxy centres, where rotation velocities are low and where estimate uncertainties are mag-

nified by the non-negligible effects of non-circular motions and of the ‘pressure’ support provided by the finite gas velocity dispersion, among other effects (see, e.g., Read et al. 2016; Pineda et al. 2017; Oman et al. 2017, for some recent work on this topic).

### 3.5 MDAR scatter

The discussion of the preceding subsection leads to the question of why, if cores are as ubiquitous as is often claimed, the scatter in the MDAR is as small as reported by McGaugh et al. (2016) and Lelli et al. (2016b). There are two reasons for this. One is that cores as large and obvious as those of NGC 3917 and IC 2574 are quite rare: indeed, most disk rotation curves only deviate mildly if at all from  $\Lambda\text{CDM}$  expectations (see, e.g., Oman et al. 2015).

The second is that the reported scatter is measured from an MDAR constructed by sampling *linearly* in radius the rotation curves of individual galaxies. This means that the inner regions are de-emphasized in the average, which is dominated by the large number of points that hover tightly around the characteristic (peak) acceleration values of each galaxy.

This is shown in the right-hand panel of Fig. 3 and is particularly obvious in the case of NGC 3917: the inner regions contribute only two points that deviate significantly from the average MDAR. The scatter in the MDAR would probably be different if each rotation curve was sampled logarithmically rather than linearly in radius. In addition, individual points in a rotation curve are not independent from each other when plotted as accelerations (i.e.,  $g_{\text{bar}}(r)$  is not

a local measure but rather depends on the whole baryonic mass profile), complicating the interpretation of the scatter.

This implies that a proper discussion of the MDAR scatter needs to include a detailed consideration of the distribution of masses, radii, and radial range sampling of galaxies in the SPARC sample. Although this exercise is beyond the goals of this paper (see Di Cintio & Lelli 2016, for a recent attempt), we note that the MDAR is a rather forgiving relation where even gross deviations from the scalings assumed in our simple model translate into relatively small changes to the predicted MDAR. This is a direct result of the narrow range of central accelerations spanned by  $\Lambda$ CDM haloes that host luminous disks, combined with the weak radial acceleration gradient of the NFW profile. This issue has been discussed in more detail in recent work (see, e.g., Santos-Santos et al. 2016; Keller & Wadsley 2016; Ludlow et al. 2016a), who used the results of direct cosmological simulations to discuss the MDAR scatter expected in  $\Lambda$ CDM.

### 3.6 Deviations from MDAR

We consider next the significance of deviations from the observed MDAR. In  $\Lambda$ CDM the MDAR has no particular meaning, and one would indeed expect systematic deviations in systems of much lower or higher mass than halos that typically host field galaxies. Examples include, at the low mass end, the haloes that host Ly- $\alpha$  absorbers at moderate redshift, and, at the massive end, rich galaxy clusters, where MOND, for example, fails to account for observations unless a dark mass component is added (Aguirre et al. 2001; Sanders 2003).

In the context of our discussion, we note that the acceleration at the centre of galaxy clusters may exceed  $a_0$ . Indeed, the central NFW acceleration peaks at  $\sim 3 \times 10^{-10} \text{ m s}^{-2}$  (i.e., three times higher than  $a_0$ ) for a cluster with  $V_{200} \sim 1500 \text{ km s}^{-1}$ , comparable to the Coma cluster. Unfortunately, galaxy cluster centres are populated by early-type galaxies, which are compact and massive enough to push the observed accelerations to even higher values. The luminous regions of these galaxies are expected therefore to populate the  $g_{\text{bar}} \approx g_{\text{tot}}$  region of the MDAR (see, e.g., Lelli et al. 2016a).

Alternatively, one might also expect strong deviations in very low surface brightness galaxies, which trace the smallest<sup>5</sup> values of  $g_{\text{bar}}$ . If such galaxies were to inhabit very massive haloes they would have high  $g_{\text{tot}}$  at low  $g_{\text{bar}}$ . Alternatively, if they were baryon-dominated, they would have  $g_{\text{tot}} \approx g_{\text{bar}}$  in the same regime, deviating in both cases substantially from the mean MDAR trend. Apparently such galaxies do not exist: very low surface brightness galaxies form preferentially in low mass haloes and are dark matter dominated.

Finally, we note that  $\Lambda$ CDM predicts a high abundance of very low mass halos where star formation has been fully prevented by cosmic reionization. These halos, however, should still be filled with (mostly ionized) gas, and may be detectable in future HI surveys (see, e.g., Benítez-Llambay

et al. 2016). Such systems should also systematically deviate from the MDAR.

## 4 SUMMARY AND DISCUSSION

Recent work has highlighted the tight relation that links the radial acceleration profile of galaxy disks,  $g_{\text{tot}}(r) = V_{\text{circ}}^2(r)/r$ , and that expected from their baryonic mass profile,  $g_{\text{bar}}(r)$ , for disk galaxies spanning a vast range of stellar mass and surface brightness. This mass discrepancy-radial acceleration relation (MDAR) indicates that few, if any, known galaxies (a) probe accelerations below a lower limit of  $a_{\text{min}} \sim 10^{-11} \text{ m s}^{-2}$ , or (b) are dark matter dominated at accelerations exceeding  $a_0 \sim 10^{-10} \text{ m s}^{-2}$ .

We have used a simple model to show that the MDAR arises naturally in  $\Lambda$ CDM. This is because (i) disk galaxies in  $\Lambda$ CDM form at the centre of dark matter haloes spanning a relatively narrow range of virial velocity (30–300  $\text{km s}^{-1}$ ); (ii) dark halo acceleration profiles are self-similar and have a broad maximum at the centre, reaching values bracketed precisely by  $a_{\text{min}}$  and  $a_0$  in that mass range; and (iii) halo mass and galaxy size scale relatively tightly with the baryonic mass of a galaxy.

This implies that accelerations exceeding  $a_0$  can *only* be reached in regions that are dominated by baryons, explaining why  $g_{\text{bar}} \approx g_{\text{tot}}$  at high acceleration. In addition, accelerations cannot fall below  $a_{\text{min}}$  because of the effective minimum halo mass needed to form a luminous galaxy, explaining why  $g_{\text{tot}} \approx a_{\text{min}}$  at the very low values of  $g_{\text{bar}}$  probed by dark matter-dominated dwarf galaxies.

Between those asymptotic limits, the MDAR follows from the tight scaling between stellar mass and halo mass implied by the baryonic physics that shapes the galaxy stellar mass function and from the observed relation between stellar mass and size. The  $g_{\text{bar}}-g_{\text{tot}}$  relation thus arises from the self-similar nature of CDM haloes and of the physical scales introduced by the galaxy formation process.

This also implies that isolated galaxies that deviate substantially from the mean  $g_{\text{bar}}-g_{\text{tot}}$  relation are difficult to account for in  $\Lambda$ CDM. Examples include the dark matter ‘cores’ inferred for some galaxies from their slowly rising inner rotation curves, which deviate from both the  $\Lambda$ CDM predictions *and* from the average MDAR (see examples in Fig. 3).

If the inferred circular velocity curves for these galaxies are correct, then they would invalidate *both* the views that the MDAR encodes a ‘fundamental law’ that goes beyond Newtonian gravity *and* that  $\Lambda$ CDM provides the framework for a correct theory of structure formation. Galaxies such as these may thus reveal potentially important modifications needed for both alternative models of gravity *and/or* for  $\Lambda$ CDM.

A simpler alternative, however, is that the inferred circular velocity curves in such galaxies are affected by substantially underestimated systematic uncertainties. This is most likely the reason for the outliers of the baryonic Tully-Fisher relation discussed as ‘missing dark matter galaxies’ by Oman et al. (2016). However, it is unclear whether such effects might be enough to bring galaxies like IC 2574 into agreement with other galaxies, and with  $\Lambda$ CDM. What is clear, however, is that such galaxies should be thoroughly

<sup>5</sup> For practical purposes  $g_{\text{bar}} \propto M_{\text{bar}}(r)/r^2$  is just a proxy for enclosed surface brightness.

and carefully examined to establish whether they constitute an insurmountable problem for  $\Lambda$ CDM or simply signal a breakdown in the methods used to infer circular velocity curves from gas velocity fields.

We end by identifying a population of galaxies where systematic deviations from MDAR are to be expected. These are the low surface brightness dwarf satellites of luminous galaxies, where tidal stripping might reduce their dark matter content and velocity dispersion while affecting little the size of the stellar component (Peñarrubia et al. 2008). Tidally-stripped dwarfs may thus dip below the ‘minimum’ acceleration ( $a_{\min}$ ) expected for isolated galaxies in  $\Lambda$ CDM. Given the strong dependence of the effects of tides on orbital time and pericentric radius, one does not expect that all satellites should be affected equally, leading to sizable scatter in the  $g_{\text{bar}}-g_{\text{tot}}$  relation at the very low surface brightness end of the satellite population. There is tentative evidence that this might indeed be the case, but a more detailed analysis is required to gauge the role of tides on the structure of satellite galaxies. Deviations from the MDAR may actually prove more revealing for our understanding of galaxy formation than the relation itself.

## 5 ACKNOWLEDGEMENTS

We acknowledge the useful comments of the referee, which helped to improve the presentation of these results. The research was supported in part by the Science and Technology Facilities Council Consolidated Grant (ST/F001166/1), and the European Research Council under the European Union’s Seventh Framework Programme (FP7/2007-2013)/ERC Grant agreement 278594-GasAroundGalaxies. CSF acknowledges ERC Advanced Grant 267291 COSMIWAY. This work used the DiRAC Data Centric system at Durham University, operated by the Institute for Computational Cosmology on behalf of the STFC DiRAC HPC Facility ([www.dirac.ac.uk](http://www.dirac.ac.uk)). The DiRAC system was funded by BIS National E-infrastructure capital grant ST/K00042X/1, STFC capital grants ST/H008519/1 and ST/K00087X/1, STFC DiRAC Operations grant ST/K003267/1 and Durham University. DiRAC is part of the National E-Infrastructure. This research has made use of NASA’s Astrophysics Data System.

## REFERENCES

- Aguirre A., Schaye J., Quataert E., 2001, *ApJ*, **561**, 550  
 Behroozi P. S., Wechsler R. H., Conroy C., 2013, *ApJ*, **770**, 57  
 Bell E. F., de Jong R. S., 2001, *ApJ*, **550**, 212  
 Benítez-Llambay A., et al., 2016, preprint, ([arXiv:1609.01301](https://arxiv.org/abs/1609.01301))  
 Bertone G., Hooper D., Silk J., 2005, *Phys. Rep.*, **405**, 279  
 Bosma A., 1978, PhD thesis, PhD Thesis, Groningen Univ., (1978)  
 Bovy J., Rix H.-W., 2013, *ApJ*, **779**, 115  
 Caldwell N., et al., 2017, *ApJ*, **839**, 20  
 Crain R. A., et al., 2015, *MNRAS*, **450**, 1937  
 Desmond H., 2016, preprint, ([arXiv:1607.01800](https://arxiv.org/abs/1607.01800))  
 Di Cintio A., Lelli F., 2016, *MNRAS*, **456**, L127  
 Famaey B., McGaugh S. S., 2012, *Living Reviews in Relativity*, **15**, 10  
 Fattahi A., et al., 2016, *MNRAS*, **457**, 844  
 Ferrero I., et al., 2016, preprint, ([arXiv:1607.03100](https://arxiv.org/abs/1607.03100))  
 Frenk C. S., White S. D. M., Davis M., Efstathiou G., 1988, *ApJ*, **327**, 507  
 Guo Q., White S., Li C., Boylan-Kolchin M., 2010, *MNRAS*, **404**, 1111  
 Kaplinghat M., Turner M., 2002, *ApJ*, **569**, L19  
 Keller B. W., Wadsley J. W., 2016, preprint, ([arXiv:1610.06183](https://arxiv.org/abs/1610.06183))  
 Kroupa P., 2012, *Publ. Astron. Soc. Australia*, **29**, 395  
 Lelli F., McGaugh S. S., Schombert J. M., Pawlowski M. S., 2016a, preprint, ([arXiv:1610.08981](https://arxiv.org/abs/1610.08981))  
 Lelli F., McGaugh S. S., Schombert J. M., 2016b, *AJ*, **152**, 157  
 Ludlow A. D., Navarro J. F., Angulo R. E., Boylan-Kolchin M., Springel V., Frenk C., White S. D. M., 2014, *MNRAS*, **441**, 378  
 Ludlow A. D., et al., 2016a, preprint, ([arXiv:1610.07663](https://arxiv.org/abs/1610.07663))  
 Ludlow A. D., Bose S., Angulo R. E., Wang L., Hellwing W. A., Navarro J. F., Cole S., Frenk C. S., 2016b, *MNRAS*, **460**, 1214  
 McGaugh S. S., 2015, *Canadian Journal of Physics*, **93**, 250  
 McGaugh S., Lelli F., Schombert J., 2016, preprint, ([arXiv:1609.05917](https://arxiv.org/abs/1609.05917))  
 Milgrom M., 1983, *ApJ*, **270**, 371  
 Moster B. P., Naab T., White S. D. M., 2013, *MNRAS*, **428**, 3121  
 Navarro J. F., Frenk C. S., White S. D. M., 1996, *ApJ*, **462**, 563  
 Navarro J. F., Frenk C. S., White S. D. M., 1997, *ApJ*, **490**, 493  
 Oh S.-H., de Blok W. J. G., Brinks E., Walter F., Kennicutt Jr. R. C., 2011, *AJ*, **141**, 193  
 Oman K. A., et al., 2015, *MNRAS*, **452**, 3650  
 Oman K. A., Navarro J. F., Sales L. V., Fattahi A., Frenk C. S., Sawala T., Schaller M., White S. D. M., 2016, *MNRAS*, **460**, 3610  
 Oman K. A., Marasco A., Navarro J. F., Frenk C. S., Schaye J., Benítez-Llambay A., 2017, preprint, ([arXiv:1706.07478](https://arxiv.org/abs/1706.07478))  
 Peñarrubia J., Navarro J. F., McConnachie A. W., 2008, *ApJ*, **673**, 226  
 Pineda J. C. B., Hayward C. C., Springel V., Mendes de Oliveira C., 2017, *MNRAS*, **466**, 63  
 Planck Collaboration et al., 2014, *A&A*, **571**, A16  
 Planck Collaboration et al., 2016, *A&A*, **594**, A13  
 Read J. I., Iorio G., Agertz O., Fraternali F., 2016, *MNRAS*, **462**, 3628  
 Rubin V. C., Thonnard N., Ford Jr. W. K., 1978, *ApJ*, **225**, L107  
 Sanders R. H., 1990, *A&ARv*, **2**, 1  
 Sanders R. H., 2003, *MNRAS*, **342**, 901  
 Santos-Santos I. M., Brook C. B., Stinson G., Di Cintio A., Wadsley J., Domínguez-Tenreiro R., Gottlöber S., Yepes G., 2016, *MNRAS*, **455**, 476  
 Sawala T., et al., 2016, *MNRAS*, **457**, 1931  
 Scarpa R., 2006, in Lerner E. J., Almeida J. B., eds, American Institute of Physics Conference Series Vol. 822, First Crisis in Cosmology Conference. pp 253–265 ([arXiv:astro-ph/0601478](https://arxiv.org/abs/astro-ph/0601478)), doi:10.1063/1.2189141  
 Schaller M., et al., 2015, *MNRAS*, **451**, 1247  
 Schaye J., et al., 2015, *MNRAS*, **446**, 521  
 Vale A., Ostriker J. P., 2004, *MNRAS*, **353**, 189  
 Walter F., Brinks E., de Blok W. J. G., Bigiel F., Kennicutt Jr. R. C., Thornley M. D., Leroy A., 2008, *AJ*, **136**, 2563  
 Wu X., Kroupa P., 2015, *MNRAS*, **446**, 330  
 van den Bosch F. C., Dalcanton J. J., 2000, *ApJ*, **534**, 146